International Journal of Pharmaceutics 396 (2010) 204–209

Contents lists available at ScienceDirect

International Journal of Pharmaceutics

journal homepage: www.elsevier.com/locate/ijpharm

Pharmaceutical Nanotechnology

Post-insertion into Lipid NanoCapsules (LNCs): From experimental aspects to mechanisms

Thomas Perrier*, Patrick Saulnier, Florian Fouchet, Nolwenn Lautram, Jean-Pierre Benoît

Inserm U646, Ingénierie de la vectorisation particulaire, Université d'Angers, 49100 Angers, France

ARTICLE INFO

Article history:
Received 10 March 2010
Received in revised form 8 June 2010
Accepted 14 June 2010
Available online 19 June 2010

Keywords:
Lipid NanoCapsules
Post-insertion
Amphiphilic phospholipids
Soft-particle analysis
Electrokinetic measurements

ABSTRACT

Over the last decade, Lipid NanoCapsules (LNCs) have been intensively used as effective drug delivery systems; they are classically prepared using a phase-inversion method. Following formulation of the LNCs, the molecular insertion of commercially-available disteraoylphosphatidylethanolamine-peg amphiphiles is performed into the LNC shell, using a post-insertion method, more classically applied with liposomes. The subsequent LNC interfacial modifications are investigated by using size and electrokinetic measurements. More particularly, the length and the nature of the hydrophilic part of the post-inserted surfactant are modified. The results are discussed in order to improve our understanding of post-insertion mechanisms.

1. Introduction

In the field of nanomedicine (drug delivery systems formulated at the nanometric scale), the nanoparticle surfaces are expected to have several different properties allowing active or passive targeting (Gupta and Gupta, 2005; Pellegrino et al., 2005; Nasongkla et al., 2006; Byrne et al., 2008) and also preventing their recognition and capture by the immune system (Fang et al., 2009). Among the available surfactants, a particular class has emerged, this being surfactants with variable amounts of polyethylene glycol (PEG). However, the introduction of such surfactants into established formulation processes forces the scientist to manipulate many parameters in order to achieve the desired structure, size range and polydispersity (Heurtault et al., 2003; Anton et al., 2007). Due to these constraints, post-formulation strategies have emerged whereby the nanoparticles are considered as platforms for interfacial modification. Organic chemistry has initiated several strategies from classical coupling reactions, such as the creation of amide (Acharya et al., 2009) and ester (Ljubimova et al., 2008) bonds, to more recent techniques based on metathesis (Koenig and Chechik, 2006; Airaud et al., 2009) or cycloadditions such as the Diels–Alder reaction (Zhu et al., 2006; Shi et al., 2009). But in most cases, these processes require the use of organic solvents and/or the use of organo-metallic compounds, which need to be removed from the sample at the end of the process. New methods such as a copper-catalysed azide–alkyne coupling reaction, known as CuAAC (Hein et al., 2008; Lutz and Zarafshani, 2008), have established water as a reference solvent for the modification of nanoparticles. To date, efforts have been made to develop re-usable and recoverable catalysts (Sirion et al., 2008).

In a similar way, physical methods have been established; in particular, post-insertion has been widely used to modify the surface of liposomes (Iden and Allen, 2001; Allen et al., 2002; Moreira et al., 2002). This consists of incubating liposomes with a micellar suspension of the added surfactant. The result is its transfer inside the liposomal, lipidic bilayer. To date, no systematic studies have been published concerning the nature of the surfactants, that is to say, the required length of the hydrophobic and hydrophilic elements, and if one or more aliphatic chain is necessary. As PEG is of great interest in pharmaceutical applications (Kim et al., 2009; Zalipsky, 1993), due to its ability to increase colloidal stability and enhance blood circulation time (Vonarbourg et al., 2006a,b) by decreasing macrophage up-take and complement activation (Vonarbourg et al., 2006a,b), we chose to use amphiphilic phospholipids-PEG to test the post-insertion process into LNCs. These surfactants have molecular weights of between 1000 to almost 6000 g/mol. Related HLB values vary from 5.44 (hydrophobic) to 17.14 (hydrophilic). Here, we propose to study the feasibility of post-insertion into LNCs and to analyse the effect of the length of the hydrophilic part. We also discuss the impact of post-insertion on the structure of the external part of LNCs by using soft-particle analysis (Ohshima, 1994, 1995, 2007), an electrokinetic method used to quantify the electrical charge density in the accessible ionic layer inside the nanoparticle shell.

* Corresponding author.
E-mail address: thomas.perrier2@hotmail.fr (T. Perrier).

0378-5173/$ – see front matter © 2010 Elsevier B.V. All rights reserved.
doi:10.1016/j.ijpharm.2010.06.019

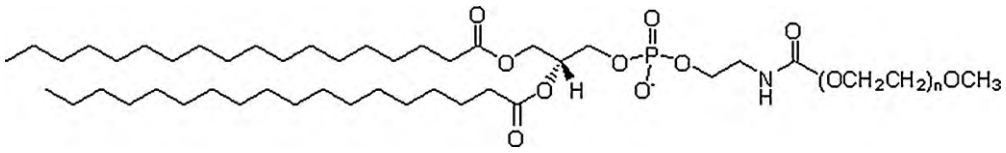

Fig. 1. Molecular structure of the phospholipid-PEGs.

Table 1
Surfactant physico-chemical parameters.

Surfactants	DSPE-PEG				
	350	750	2000	3000	5000
MW of surfactants (g/mol)	1131	157	2805	3774	5801
Nb of PEG units	7	16	45	67	113
MW of PEG (g/mol)	308	704	1980	2948	4972
HLB	5.44	9.21	14.11	15.61	17.14

2. Experimental

2.1. Materials

Labrafac® WL 1349 (Gattefossé S.A., Saint-Priest, France) is a mixture of capric and caprylic acid triglycerides. NaCl was purchased from Prolabo (Fontenay-sous-Bois, France) and water was obtained from a Milli-Q-plus® system (Millipore, Paris, France). Lipoïd® S75-3 (Lipoïd GmbH, Ludwigshafen, Germany) is a soybean lecithin made of 69% of phosphatidylcholine, 10% phosphatidylethanolamine and other phospholipids, and Solutol® HS 15 (BASF, Ludwigshafen, Germany) is a mixture of free polyethylene glycol 660 (PEG) and polyethylene glycol 660 hydroxystearate. The dialysis membrane was purchased from Spectrapore and has a molecular weight cut-off point equal to 100,000 Da.

1,2-Distearoyl-*sn*-glycero-3-phosphoethanolamine-*N*-[methoxy(polyethylene-glycol)] (see Fig. 1) with a peg length of between 350 and 5000 g mol^{-1} (see Table 1), corresponding to 7–113 units of PEG, was supplied by Avanti® Polar Lipids Inc. (Alabaster, USA).

The hydrophilic lipophilic balance (HLB) was calculated according to Griffin's formula (Griffin, 1949, 1954, 1979):

$$\mathrm{HLB} = \frac{20 m_W}{M} \quad (1)$$

where m_W is the molecular weight of PEG and M is the molecular weight of the whole molecule.

2.2. Preparation of Lipid NanoCapsules (LNCs)

This formulation method has already been well documented (Heurtault et al., 2002a,b) and can be briefly presented as follows: all components (Solutol HS-15, Lipoïd S75-3, sodium chloride, Labrafac CC and water) are mixed under magnetic stirring at an agitation speed of 200 rpm at room temperature leading to an O/W emulsion. After progressive heating at 4 °C/min, a short interval of transparency at temperatures close to 70 °C can be observed, and the inverted phase (water droplets in oil) is obtained at 85 °C. At least three temperature cycles alternating from 60 to 85 °C at the same rate are applied near the phase-inversion zone. Thereafter, the mixture undergoes a fast cooling-dilution process: it is diluted 1:3.5 with 12.5 ml of cold water at 2 °C and stirred for 30 min, leading to the formation of an LNC suspension of the desired size. LNCs are liquid core nanocapsules made of medium-chain triglycerides (Labrafac CC) surrounded by a surfactant shell assembled in a mixed monolayer of Solutol HS-15 and Lipoïd S75-3.

2.3. Preparation of post-inserted LNCs

To reach a high density of PEG at the surface, 1.75 ml LNC (10^{15} particles/ml) (Minkov et al., 2005) were incubated for 105 min at 60 °C with 1.3 ml of aqueous micellar solution (variable concentration) of 1,2-distearoyl-*sn*-glycero-3-phosphoethanolamine-*N*-[methoxy(polyethylene-glycol)] (DSPE-PEG$_{2000}$-OCH$_3$) supplied by Avanti® Polar Lipids Inc. (Alabaster, USA), as shown in Fig. 2. The suspension was vortexed every 15 min and then quenched in an ice bath for 1 min. The final DSPE-PEG concentration corresponded to 10 mol% of total surface molecules, as shown in Fig. 2.

2.4. Analysis of the relationship between time and temperature on the post-insertion process

To determine the effect of temperature on the post-insertion process, we performed post-insertion with the same LNC batch at

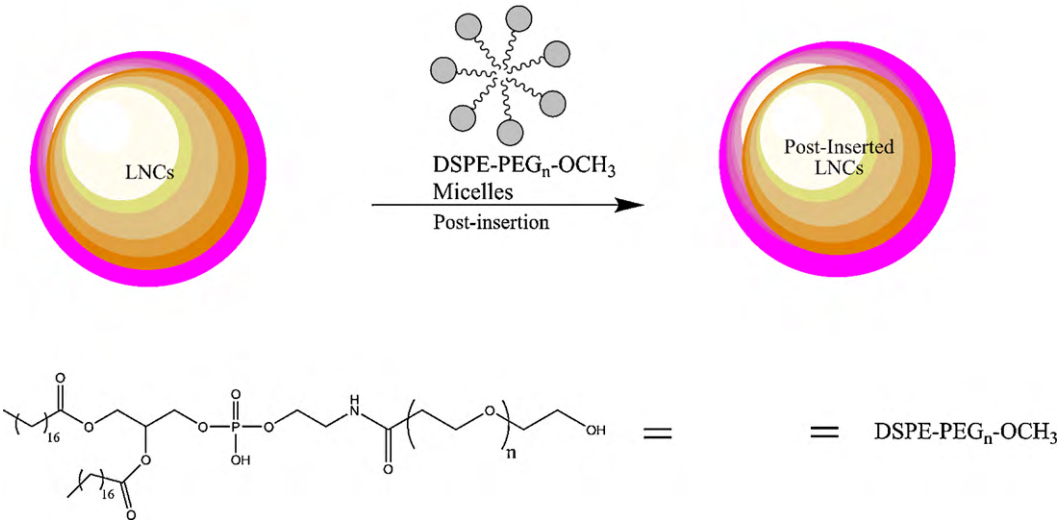

Fig. 2. Post-insertion protocol.

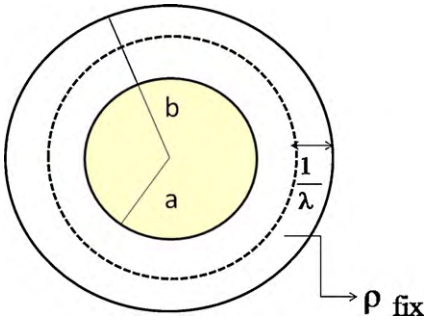

Fig. 3. Schematic illustration of a soft particle.

temperatures between 25 and 60 °C. Dynamic light scattering measurements were carried out every 5 min to follow the post-insertion process.

2.5. LNC size and zeta potential distribution

All particles were characterised in terms of size and zeta potential using a NanoZS apparatus (Malvern Instruments) after the dispersion of 50 μl of the mother suspension in 3 ml of the aqueous medium. Each measurement (size and zeta potential) was carried out in triplicate. All experiments were carried out at 25 °C and with similar conductivity values.

2.6. Electrokinetic measurements: soft-particle analysis

To determine the electrokinetic behaviour of LNCs according to the soft-particle theory (Ohshima, 1994, 1995, 2007), we performed electrophoretic mobility measurements using NanoZS instruments. 50 μl samples (LNCs) were diluted into sodium chloride solution with variable concentrations up to 40 mol/m^3. Reported values are the mean of five measurements. Experimental values were fitted by using the following Eq. (2):

$$\mu = \frac{\varepsilon_r \varepsilon_0}{\eta} \frac{(\psi_0/\kappa_m) + (1/\lambda)\psi_{DON}}{(1/\kappa_m) + (1/\lambda)} + \frac{\rho_{fix}}{\eta}\left(\frac{1}{\lambda}\right)^2 \quad (2)$$

where ψ_0 is the potential for $r = b$ and ψ_{DON} is the Donnan potential in the polyelectrolyte layer (see Fig. 3). Both are calculated according to Eqs. (3) and (4). κ_m and κ are given by Eqs. (5) and (6).

$$\psi_0 = \psi_{DON} + \frac{2nkT}{\rho_{fix}}\left\{1 - \left[\left(\frac{\rho_{fix}}{2zne}\right)^2 + 1\right]^{1/2}\right\} \quad (3)$$

$$\psi_{DON} = \frac{kT}{ze}\ln\left\{\frac{\rho_{fix}}{2zne} + \left[\left(\frac{\rho_{fix}}{2zne}\right)^2 + 1\right]^{1/2}\right\} \quad (4)$$

$$\kappa_m = \kappa\sqrt[4]{1 + \left(\frac{\rho_{fix}}{2zne}\right)^2} \quad (5)$$

κ is the Debye length and is calculated using:

$$\kappa = \sqrt{\frac{\sum_{i=1}^{N} z_i^2 e^2 n_i}{\varepsilon_0 \varepsilon_r kT}} \quad (6)$$

ε_0: electric permittivity of free space; ε_r: electric permittivity of water; T: temperature; z_i: charge number of ion species i; z: charge number of the electrolyte (supposed to be symmetrical); e: elemental charge. k: Boltzmann's constant; n: bulk electrolyte molar concentration; n_i: bulk ion i molar concentration; N: charge unit molar concentration in the LNC shell; ρ_{fix}: pseudo charge density in the electrolyte accessible layer; λ^{-1}: depth of the accessible layer. According to Fig. 3, the particles have a core of radius 'a' surrounded by a polyelectrolyte layer (depth $b - a$). $1/\lambda$ represents the accessible depth accessible to ions (Na^+, Cl^-) inside the polyelectrolyte layer; these interact with the ethylene oxide dipoles constituting the PEG units through the well-known Lifshitz–Van Der Walls interactions.

3. Results

Narrow size distributions are easily obtained (PDI < 0.1) and in this case we chose to work with LNCs with a 55 nm hydrodynamic diameter (H_D). As LNC shells contain hydrophilic surfactant with PEG chains, Solutol HS-15, LNCs display a zeta potential equal to −10 mV, identical to the previously-obtained value (Vonarbourg et al., 2005) and very close to the zeta potential (ZP) of other pegylated carriers such as liposomes (Yang et al., 2007). Post-insertion experiments were carried out by incubating the micellar suspension of DSPE-PEG$_{2000}$-OCH$_3$ with the LNCs. The amount of DSPE-PEG$_{2000}$-OCH$_3$ was chosen between 0 and 10% (% in Mol of Lipoïd S75-3 and Solutol HS-15) in order to analyse the effect on LNC size distribution and zeta potential.

Fig. 4a and b present the evolution of H_D and ZP versus the concentration of DSPE-PEG$_{2000}$-OCH$_3$. The H_D increases from 55 to 70 nm, corresponding to a 27% increase, if the percentage of DSPE-PEG$_{2000}$-OCH$_3$ is 5%. When [DSPE-PEG$_{2000}$-OCH$_3$] is higher than 5%, the H_D does not increase, and 70 nm seems to be the limit. In all experiments, the polydispersity index (PDI) was lower than 0.2. The ZP, measured in similar conditions, clearly decreased with the amount of DSPE-PEG$_{2000}$-OCH$_3$ with a linear relationship.

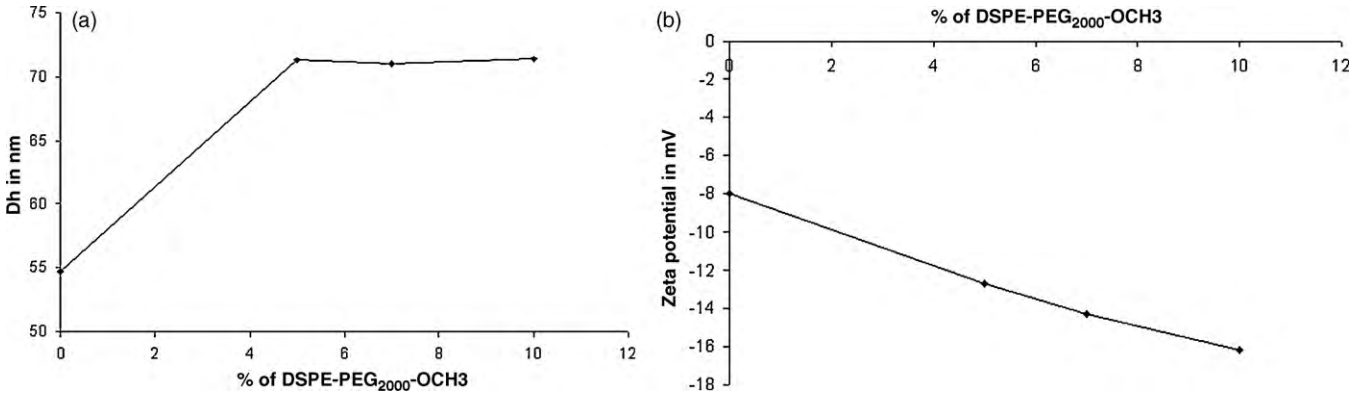

Fig. 4. (a and b) Variation of H_D and ZP with the amount of DSPE-PEG$_{2000}$-OCH$_3$.

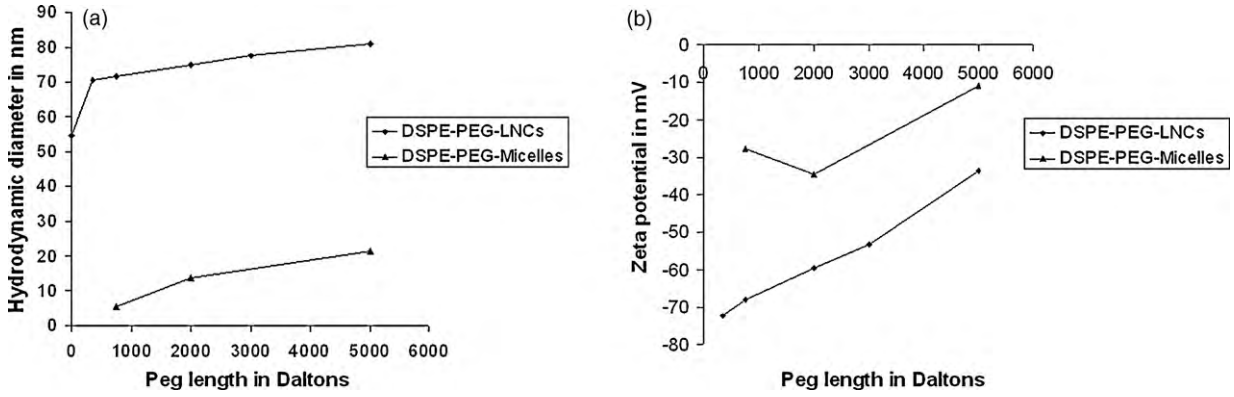

Fig. 5. (a and b) Variation of H_D and PZ for post-inserted LNCs and DSPE-PEG micelles.

Control experiments were carried out by treating LNCs under similar conditions of temperature and salinity as those related to the post-insertion, but without the addition of DSPE-PEG_{2000}-OCH_3. They clearly show no modification of H_D and ZP levels (results not shown). This indicates that LNCs are not modified under these experimental post-insertion conditions. Thus, variations of H_D and ZP values correspond to a shell incorporation of DSPE-PEG_{2000}-OCH_3 molecules. Further experiments were carried out at a constant molar amount of DSPE-PEG_X-OCH_3 with a variation of the length of PEG moiety. Fig. 5a and b shows the evolution of H_D and ZP for post-inserted LNCs with the selected surfactants. H_D increases with the length of the PEG chain, following a linear progression versus PEG length, ranging from 350 to 5000 g mol^{-1}.

This progression is close to that observed for DSPE-PEG-micelles, as previously reported in the literature (Sezgin et al., 2006). Concerning ZP variations, negative values (−72 mV) were obtained for the shortest PEG chains. From this extreme point, ZP values decrease in linear fashion with PEG length until −33 mV for PEG_{5000}.

In order to determine both the pseudo-charge density and the accessibility to ions, we performed electrokinetic experiments for each post-inserted LNC. Fig. 6 shows the variations of experimental electrophoretic mobility (marked points) versus the sodium chloride concentration. In all cases, electrophoretic mobility (from -6×10^{-8} to almost 0 $m^2/V\,s$) corresponded to hyperbolic variations versus [NaCl]. It is obvious that strong differences occur for LNC electrokinetic behaviour versus PEG length. For example, electrophoretic mobility, for high [NaCl] levels, is close to 3×10^{-8} $m^2/V\,s$ for PEG_{350} and is almost zero for PEG_{5000}.

Theoretical values (continuous lines) were calculated using Eq. (1). The concordance between the theoretical and experimental

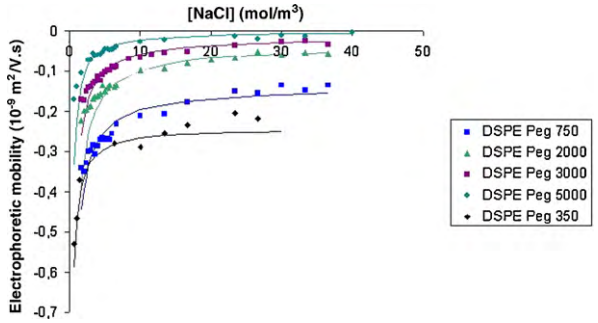

Fig. 6. Electrokinetic measurements for post-inserted LNCs.

curves was obtained after modification of the fitting parameters ρ_{fix} and $1/\lambda$.

Subsequently, the different adjusting parameter (ρ_{fix} and $1/\lambda$) values were determined. Their related variations are presented in Fig. 7a and b as a function of PEG length.

ρ_{fix} presents minimal values for PEG_{2000}, -12.8×10^{-5} C/m^3. $1/\lambda$ clearly decreases with the PEG length (10.7 nm for PEG_{350} to 0.1 nm for PEG_{5000}). The error bars depend on the desired correlation between experimental and theoretical results. We chose 10% relative error for each value.

4. Discussion

Starting from the formulation of LNCs, we have demonstrated that we can apply post-insertion for the modification of the outer part of LNCs. An incubation time of at least 100 min, and a tem-

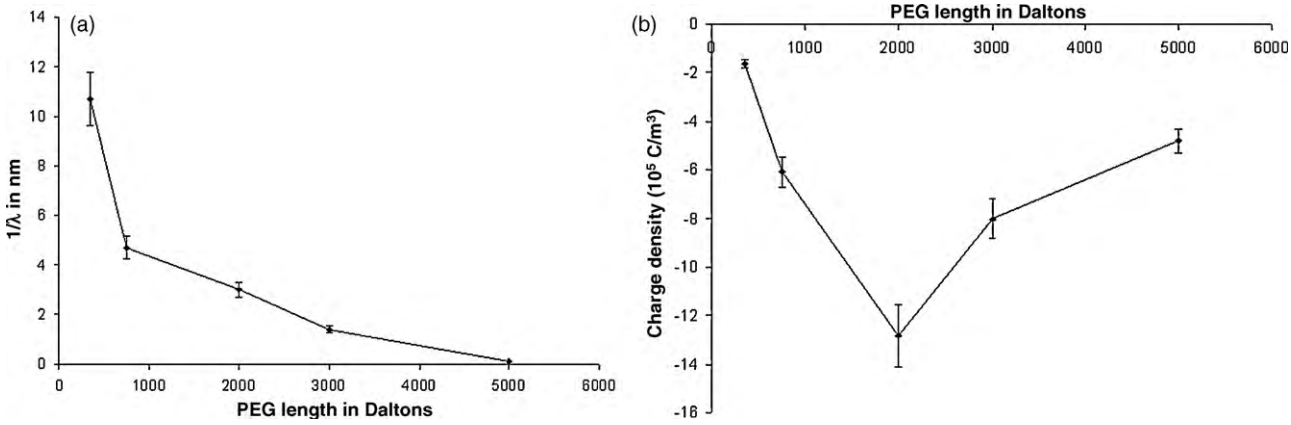

Fig. 7. (a and b) Pseudo-charge density ρ_{fix} and depth ($1/\lambda$) of the electrolyte penetrating layer.

Table 2
Relationship between temperature and post-insertion duration.

Post-insertion temperature (°C)	Time to reach completion
25	No post-insertion
37	240 min
45	180 min
60	90 min

perature of around 60 °C have been found to be necessary in order to see changes in dynamic light scattering and zeta potential measurements (Table 2).

An increase in H_D levels cannot be explained by the classical absorption of DSPE-PEG_{2000}-OCH_3 micelles ($H_{Dmicelles}$ around 15 nm) onto LNCs, since micelle absorption should produce LNCs with higher H_D values (at least equal to 55 nm + $2H_{Dmicelles}$). Experimental results indicate that DSPE-PEGs are transferred from micelles to LNCs during the process. On the other hand, since ZP is a linear function of the amount of DSPE-PEG_{2000}-OCH_3, the post-insertion can be interpreted as a molecular insertion of DSPE-PEG_{2000}-OCH_3 into the LNC shell. The post-insertion outcome is a temperature-dependent molecular transfer. ZP variations can be attributed to the increase of pseudo or apparent charges, when the global dipolar moment varies following the density and the spatial repartition of the ethylene oxide units coming from the transferred molecules. Therefore we can conclude that the ionic distribution inside the Stern layer and consequently the ZP is highly dependent on this statistical, dipolar distribution. Control experiments (results not shown) indicate that the H_D increase cannot be interpreted as classical Ostwald ripening or the coalescence of LNCs, independent of post-insertion phenomena. If this is the case, we should obtain respectively H_R^3 (H_R: hydrodynamic radius) and $1/H_R^2$ variations against time (Taylor, 1998; Izquierdo et al., 2002). In our studies, H_R^3 and $1/H_R^2$ do not vary over a time period greater than many weeks, even at a temperature close to 60 °C.

For amounts of DSPE-PEG up to 5%, H_D values remain constant. This is not the case for the ZP values, thereby indicating that additional DSPE-PEG molecules are still interacting with the LNC. Nevertheless, for this concentration range, these molecules can easily be removed by simple dialysis (results not shown).

Nevertheless, H_D values are lower than those predicted with an assumption of linear conformation of PEG (brush structure). In other words, if we consider a length of 0.15 nm for a carbon–carbon bond and a length of 0.14 nm for a carbon–oxygen bond, the length of PEG moieties (in linear conformation) should produce post-inserted LNCs with higher H_D values (the number of carbon–carbon and carbon–oxygen bonds are multiplied by the length of each bond, respectively), around 80 nm for DSPE-PEG2000. This indicates that PEG chains interact strongly in a compact conformation, surely similar to a mushroom shape.

In the second set of experiments, the shape of the curves describing the evolution of H_D with PEG length follows the one obtained for DSPE-PEG micelles. The ZP values, for each post-inserted LNC, are different from the ZP of DSPE-PEG micelles; this indicates a synergic contribution between ethylene oxide dipoles of both Solutol HS-15 and additional DSPE-PEGs. Here also, the measured ZP values are the result of several factors: the number of ethylene oxide units, the electronic density and the dipolar distribution within the active region. To underline these facts, post-insertion with DSPE-PEG_{350}-OCH_3 produces LNCs with ZP values equal to −72 mV, much more negative than that measured for DSPE-PEG_{5000}-OCH_3 (−33 mV) and for DPSE-PEG_{350}-OCH_3 micelles (−28 mV). DSPE-PEG_{350}-OCH_3 is shorter than Solutol HS-15 (PEG 660), and post-insertion produces LNCs with a high density of dipolar moments confined in a small volume. The electronic density is increased and, at the same time the ZP value decreases. On the other hand, DSPE-PEG_{5000}-OCH_3 is longer than Solutol HS-15 and the ZP value is only the result of the external part of the whole PEG moiety. Similar considerations can be conducted for experiments with DSPE-$PEG_{750,\ 2000}$ and $_{3000}$.

In order to detail the robustness of post-inserted LNCs, dialysis was carried out on each batch. H_D levels increased after dialysis due to changes in the hydration of PEG chains, since dialysis was conducted with salt-free water. The PEG chains were found to be a little bit loose, involving a small increase of H_D. One particular case is for DSPE-PEG_{5000}-OCH_3, since the H_D decreases after dialysis. Considering that this surfactant is very hydrophilic (HLB = 17.14), post-insertion should be partially reversible. In addition, to see if other surfactants could be used, we tried post-insertion with Solutol HS-15 micelles instead of DSPE-PEG_{2000}-OCH_3 ones. No modification of H_D and ZP levels could be obtained, even though Solutol HS-15 has HLB values (between 14 and 16) close to those of DSPE-PEG_{2000}-OCH_3. This fact indicates that the hydrocarbon part should be composed of at least two aliphatic chains. We tried post-insertion with Solutol HS-15 micelles and with cholesterol-PEG_{660} (results not shown); no variation of H_D and ZP values was detected under the same experimental conditions. These additional experiments indicate that post-insertion is not possible with these surfactants, even if their molecular structure is similar to DSPE-PEG_{750}. For each PEG length, post-inserted LNCs behave as soft particles and can be considered as hairy, spherical nanoparticles.

In order to detail the relationship between PEG conformation and the ZP measurements, we applied soft-particle analysis as previously described. In a general way, if the [NaCl] concentration is low, the apparent charge of LNCs is high, and the LNCs are found to be mobile in the applied electric field. On the contrary, if the [NaCl] concentration is high, the apparent charge of LNCs is balanced by ions (ion dipole interactions), and subsequently LNCs are less sensitive to the external electric field. Fitting procedures allowed us to determine two main parameters: the electronic density ρ_{fix} (C/m^3) and the accessibility to ions into the shell $1/\lambda$ (nm). $1/\lambda$ decreases when PEG length increases in relation with much higher levels of intermolecular interaction, until the counter-ions can penetrate the LNC shells. Long PEG chains rigidify the LNC shells since $1/\lambda$ is very small ($1/\lambda$ also provides resistance to the hydrodynamic flow).

This method shows that, without any doubt, DSPE-PEG_{2000} molecules promote the best intermolecular arrangement at the interface of the LNCs, as indicated by the maximum level of the pseudo-charge density. In this case, one can suppose high levels of enthalpic distribution of PEG chains without intermolecular dipolar compensation.

5. Conclusion

This work demonstrates that post-insertion works as well on LNCs as on liposomes. Furthermore, it proposes a method for the setting-up of post-insertion feasibility domains. From these experimental constraints, several important points arise: since post-insertion is a temperature-dependent process, variations of lipid fluidity on the surface of LNCs, changes in lipid solubility, and the conformation of PEG chains from Solutol HS-15, should favour the transfer of DSPE-PEG molecules from micelles to LNCs. On the basis of the literature, and our own experience, DSPE-PEG molecules have to be associated into micelles in order for post-insertion to occur. Initial experiments have established a base for finding optimal post-insertion conditions. It is obvious that the maximum amount of inserted DSPE-PEG has to be fixed. In our case, this value was found to be between 5 and 10% of the amount of surfactant forming the shell. This experiment establishes a limit for the density of inserted molecules. It is also necessary to highlight that post-insertion conditions can be adapted to specific constraints: in the case of thermo-sensitive groups, the post-insertion temperature can be diminished, though more time is required.

The second batch of experiments, with the variation of PEG length and the subsequent purification by dialysis, allowed us to fix the limits for post-insertion in terms of the nature of transferred amphiphiles. Both low-HLB and high-HLB surfactants can be used for post-insertion. But, in the case of highly hydrophilic molecules, post-insertion should be reversible and incomplete. Furthermore, the dipolar distribution provided by zeta potential and electrokinetic measurements indicates that the conformation of the PEG chains is not the same for low-HLB and high-HLB amphiphiles. One can easily understand the impact of this fact for the use of post-inserted LNCs. As accessibility to ions decreases with PEG length, and since the conformation of PEG tends to be globular, the length of PEG should be adapted for each application. For example, if shell accessibility is important (as in chemical grafting, organ targeting, etc.) a PEG with a length of 2000 or 3000 g mol^{-1} is well suited. On the other hand, if LNCs have to be protected from the external medium, longer PEG lengths are required.

Interfacial experiments are currently being conducted to assess the molecular packing of Solutol HS-15 and Lipoïd S75-3 in relation to temperature.

Acknowledgments

We wish to thank European Union (Project Nanoear) and the *Région Pays de la Loire* for providing financial support for this work. We are grateful to Dr. Guillaume Bastiat for helping us with the use of fitting software and for providing useful advice.

References

Acharya, S., Dilnawaz, F., Sahoo, S.K., 2009. Targeted epidermal growth factor receptor nanoparticle bioconjugates for breast cancer therapy. Biomaterials 30, 5737–5750.

Airaud, C., Ibarboure, E., Gaillard, C., Héroguez, V., 2009. Nanostructured polymer composite nanoparticles synthesized in a single step via simultaneous ROMP and ATRP under microemulsion conditions. J. Polym. Sci. Part A: Polym. Chem. 47, 4014–4027.

Allen, T.M., Sapra, P., Moase, E., 2002. Use of the post-insertion method for the formation of ligand-coupled liposomes. Cell. Mol. Biol. Lett. 7, 217–219.

Anton, N., Saulnier, P., Béduneau, A., Benoit, J.-P., 2007. Salting-out effect induced by temperature cycling on a water/nonionic surfactant/oil system. J. Phys. Chem. B 111, 3651–3657.

Byrne, J.D., Betancourt, T., Brannon-Peppas, L., 2008. Active targeting schemes for nanoparticle systems in cancer therapeutics. Adv. Drug Deliv. Rev. 60, 1615–1626.

Fang, C., Bhattarai, N., Sun, C., Zhang, M., 2009. Functionalized nanoparticles with long-term stability in biological media. Small 5, 1637–1641.

GRIFFIN, W.C.J., 1949. Soc. Cosmet. Chem. 1, 311.

GRIFFIN, W.C.J., 1954. Soc. Cosmet. Chem. 5, 4.

Griffin, W.C.J., 1979. Kirk-Othmer Encyclopedia of Chemical Technology, vol. 8., 3rd ed. J. Wiley & Sons, New York, 900 and 620.

Gupta, A.K., Gupta, M., 2005. Synthesis and surface engineering of iron oxide nanoparticles for biomedical applications. Biomaterials 26, 3995–4021.

Hein, C.D., Liu, X.-M., Wang, D., 2008. Click chemistry, a powerful tool for pharmaceutical sciences. Pharm. Res. 25, 2216–2230.

Heurtault, B., Saulnier, P., Pech, B., Proust, J.E., Benoît, J.P., 2002a. Properties of polyethylene glycol 660 12-hydroxy stearate at a triglyceride/water interface. Int. J. Pharm. 242, 167–170.

Heurtault, B., Saulnier, P., Pech, B., Proust, J.-E., Benoit, J.-P., 2002b. A novel phase inversion-based process for the preparation of lipid nanocarriers. Pharm. Res. 19, 875–880.

Heurtault, B., Saulnier, P., Pech, B., Venier-Julienne, M.-C., Proust, J.-E., Phan-Tan-Luu, R., Benoît, J.-P., 2003. The influence of lipid nanocapsule composition on their size distribution. Eur. J. Pharm. Sci. 18, 55–61.

Iden, D.L., Allen, T.M., 2001. In vitro and in vivo comparison of immunoliposomes made by conventional coupling techniques with those made by a new post-insertion approach. Biochim. Biophys. Acta Biomembr. 1513, 207–216.

Izquierdo, P., Esquena, J., Tadros, Th.F., Dederen, C., Garcia, M.J., Azemar, N., Solans, C., 2002. Formation and stability of nano-emulsions prepared using the phase inversion temperature method. Langmuir 18, 26–30.

Kim, J.-Y., Kim, J.-K., Park, J.-S., Byun, Y., Kim, C.-K., 2009. The use of PEGylated liposomes to prolong circulation lifetimes of tissue plasminogen activator. Biomaterials 30, 5751–5756.

Koenig, S., Chechik, V., 2006. Shell cross-linked Au nanoparicles. Langmuir 22, 5168–5173.

Ljubimova, J.Y., Fujita, M., Ljubimov, A.V., Torchilin, V.P., Black, K.L., Holler, E., 2008. Poly(malic acid) nanoconjugates containing various antibodies and oligonucleotides for multitargeting drug delivery. Nanomedicine 3, 247–265.

Lutz, J.-F., Zarafshani, Z., 2008. Efficient construction of therapeutics, bioconjugates, biomaterials and bioactive surfaces using azide–alkyne "click" chemistry. Adv. Drug Deliv. Rev. 60, 958–970.

Minkov, I., Ivanova, T., Panaiotov, I., Proust, J., Saulnier, P., 2005. Reorganization of lipid nanocapsules at air-water interface: I. Kinetics of surface film formation. Colloids Surf. B 45, 14–23.

Moreira, J.N., Ishida, T., Gaspar, R., Allen, T.M., 2002. Use of the post-insertion technique to insert peptide ligands into pre-formed stealth liposomes with retention of binding activity and cytotoxicity. Pharm. Res. 19, 265–269.

Nasongkla, N., Bey, E., Ren, J., Ai, H., Khemtong, C., Guthi, J.S., Chin, S.-F., Sherry, A.D., Boothman, D.A., Gao, J., 2006. Multifunctional polymeric micelles as cancer-targeted, MRI-ultrasensitive drug delivery systems. Nano Lett. 6, 2427–2430.

Ohshima, H., 1994. Electrophoretic mobility of soft particles. J. Colloid Interf. Sci. 163, 474–483.

Ohshima, H., 1995. Electrophoresis of soft particles. Adv. Colloid Interface Sci. 62, 189–235.

Ohshima, H., 2007. Electrokinetics of soft particles. Colloid Polym. Sci. 285, 1411–1421.

Pellegrino, T., Kudera, S., Liedl, T., Javier, A.M., Manna, L., Parak, W.J., 2005. On the development of colloidal nanoparticles towards multifunctional structures and their possible use for biological applications. Small 1, 48–63.

Sezgin, Z., Yüksel, N., Baykara, T., 2006. Preparation and characterization of polymeric micelles for solubilization of poorly soluble anticancer drugs. Eur. J. Pharm. Biopharm. 64, 261–268.

Shi, M., Ho, K., Keating, A., Shoichet, M.S., 2009. Doxorubicin-conjugated immunonanoparticles for intracellular anticancer drug delivery. Adv. Funct. Mater. 19, 1689–1696.

Sirion, U., Yu, J.B., Byoung, S.L., Dae, Y.C., 2008. Ionic polymer supported copper(I): a reusable catalyst for Huisgen's 1,3-dipolar cycloaddition. Synlett, 2326–2330.

Taylor, P., 1998. Ostwald ripening in emulsions. Adv. Colloid Interf. Sci. 75, 107–163.

Vonarbourg, A., Saulnier, P., Passirani, C., Benoit, J.-P., 2005. Electrokinetic properties of noncharged lipid nanocapsules: influence of the dipolar distribution at the interface. Electrophoresis 26, 2066–2075.

Vonarbourg, A., Passirani, C., Saulnier, P., Benoit, J.-P., 2006a. Evaluation of pegylated lipid nanocapsules versus complement system activation and macrophage uptake. Biomaterials 27, 4356–4373.

Vonarbourg, A., Passirani, C., Saulnier, P., Simard, P., Leroux, J.C., Benoit, J.P., 2006b. Parameters influencing the stealthiness of colloidal drug delivery systems. J. Biomed. Mater. Res. Part A 78, 620.

Yang, T., Choi, M.-K., Cui, F.-D., Kim, J.S., Chung, S.-J., Shim, C.-K., Kim, D.-D., 2007. Preparation and evaluation of paclitaxel-loaded PEGylated immunoliposome. J. Control. Release 120, 169–177.

Zalipsky, S., 1993. Synthesis of an end-group functionalized polyethylene glycol-lipid conjugate for preparation of polymer-grafted liposomes. Bioconjugate Chem. 4, 296–299.

Zhu, J., Kell, A.J., Workentin, M.S., 2006. A retro-Diels–Alder reaction to uncover maleimide-modified surfaces on monolayer-protected nanoparticles for reversible covalent assembly. Org. Lett. 8, 4993–4996.